High Precision Sensor for High Values of Relative Humidity

(Based on Polymer-Coated STW Resonant Device)

*P. Bruno[1], G. Cicala[2], F. Corsi[3], **A. Dragone**[3], A.M. Losacco[4]*

[1]Dipartimento di Chimica - Università di Bari
[2]IMIP-CNR w/o Dipartimento di Chimica - Università di Bari
[3]Politecnico di Bari – Dipartimento di Elettrotecnica ed Elettronica
[4]Centro Laser S.C.R.L. - Valenzano

DIPARTIMENTO DI CHIMICA
UNIVERSITA' DI BARI

C.N.R. - I.M.I.P.
BARI

Outline

- Why a sensor for high relative humidity ranges?
- How does our sensor work?
  - The acoustic device
  - The sensing mechanism
- Experiment set-up
- Results
- Front-end electronics
- Conclusions

Why high relative humidity ranges?

Fog dissipation systems by nitrogen

Actual monitoring systems to be optimized in size and cost

A new high relative humidity range sensor based on polymer-coated STW resonant device

A fog dissipation system

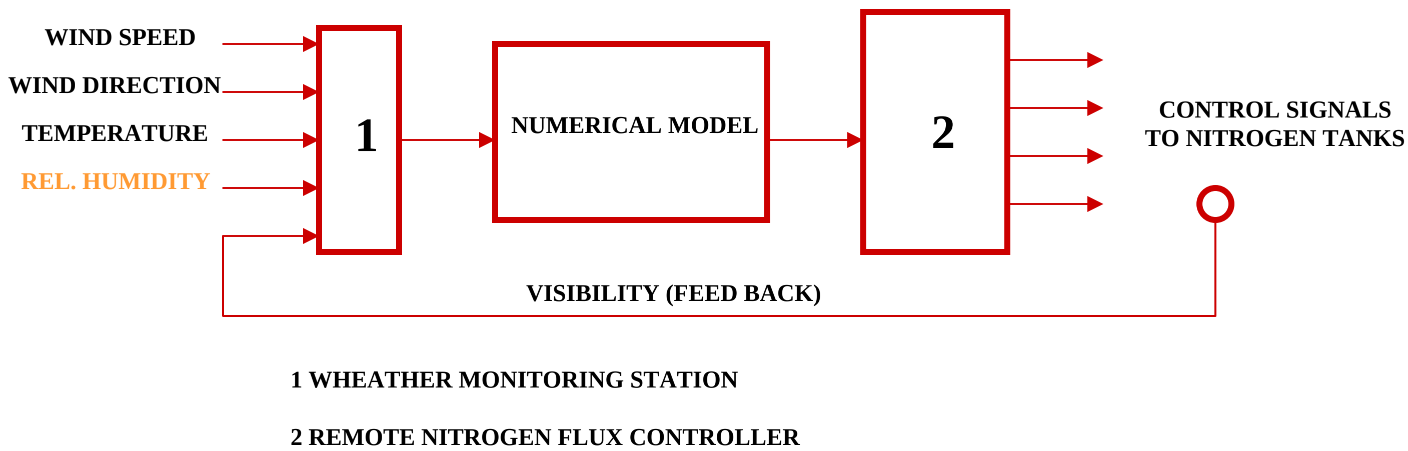

Block diagram of the automatic fog dissipation system installed and tested at the Venezia Est tollhouse, Italy (Central Aerological Observatory, Russia and Autovie Venete, Italy)

An example

Bankova, Koloskov, Krasnoskaya, Sergeeev, Cherinkov, Pani, Ferrante,
Proceedings of the 8th WMO Scientific Conference on Weather Modification, Casablanca (7-12/4/2003)

Humidity sensors

Humidity sensors

Direct

Measure of the Relative Humidity
i.e. The amount of water vapor in the atmosphere, expressed as a percentage of the maximum quantity that could be present at a given temperature.

Indirect

Measure of the Dew Point
i.e. the temperature to which air must be cooled at a constant pressure to become saturated and condense upon a solid surface.

Relations between Relative Humidity and Dew Point

$$T_d = b\frac{B}{1-B}$$

$$B = \frac{\log\left(\frac{RH}{100}\right) + \frac{aT}{b+T}}{a}$$

$$RH = 10^{\frac{ab(T_d - T)}{(b+T_d)(b+T)}}$$

a=7,5 and b=237,3 for T>0

Commercial Humidity sensors

Resistive
(direct)

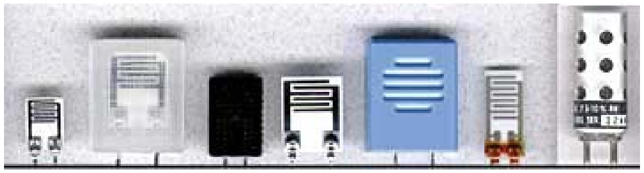

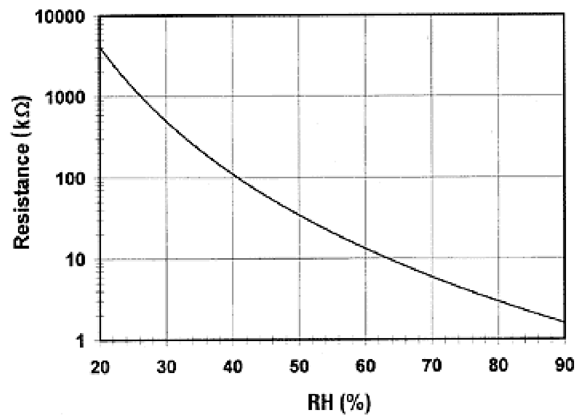

Abs error 2%, Insensitive above 90%,
Response Time 10s-30s (63% RH step)

Capacitive
(direct)

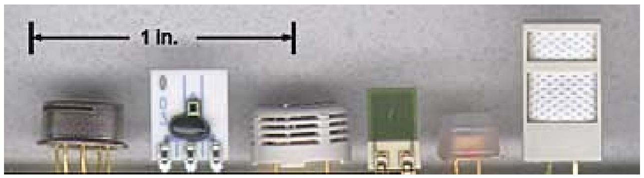

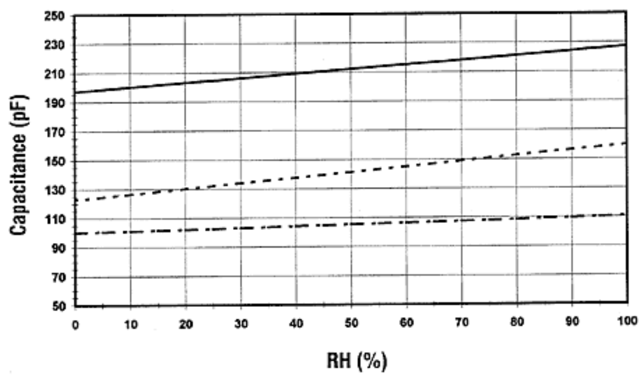

Abs error 2%, Low sensitivity above 90%
Response Time 30s-60s (63% RH step)

Commercial Humidity sensors

Chilled Mirror

(Indirect)

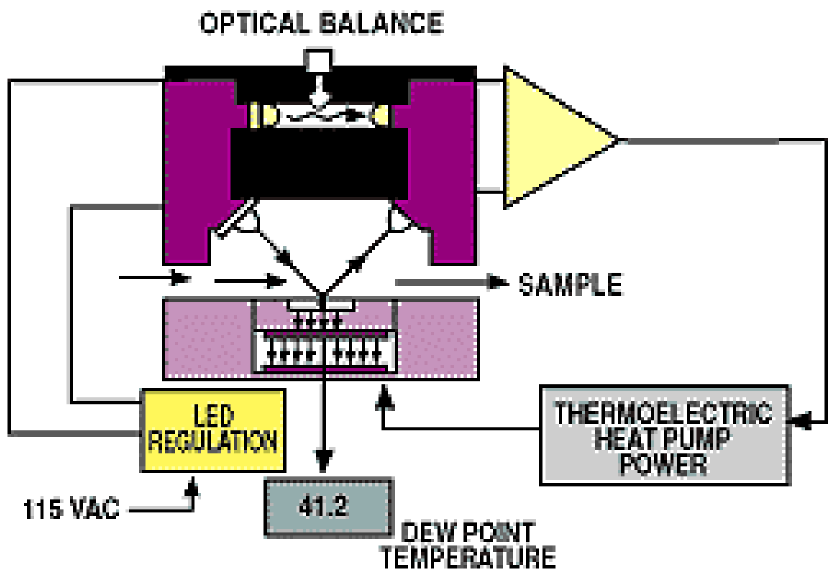

Abs error 0.2°C, Response Time 10s-30s (63% RH step)

Outline

- A sensor for high relative humidity ranges
- How does our sensor work?
  - The acoustic device
  - The sensing mechanism
- Experiment set-up
- Results
- Front-end electronics
- Conclusions

How does it work?

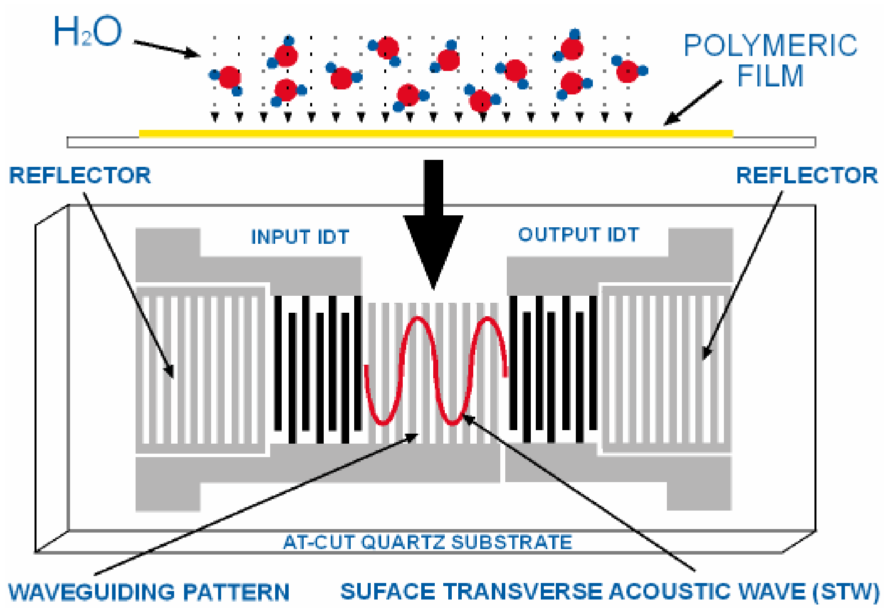

a. **The polymeric film absorbs water molecules.**
b. **The increase of the load on the device surface turns into a decrease of the STW propagation velocity.**
c. **Down-shift of the device resonance frequency.**

Acoustic Modes

SAW

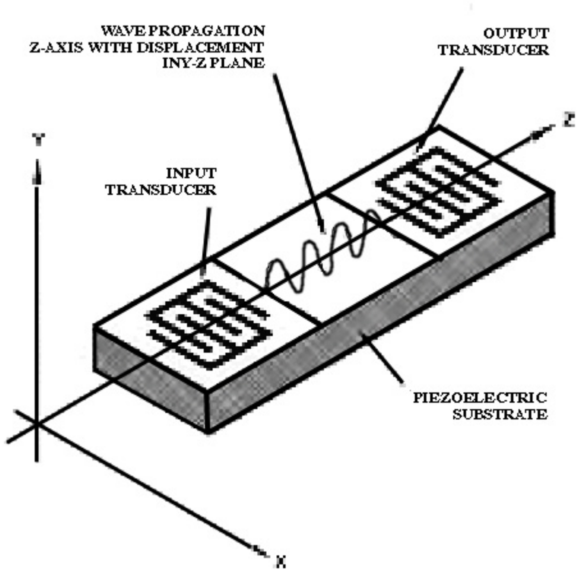

STW

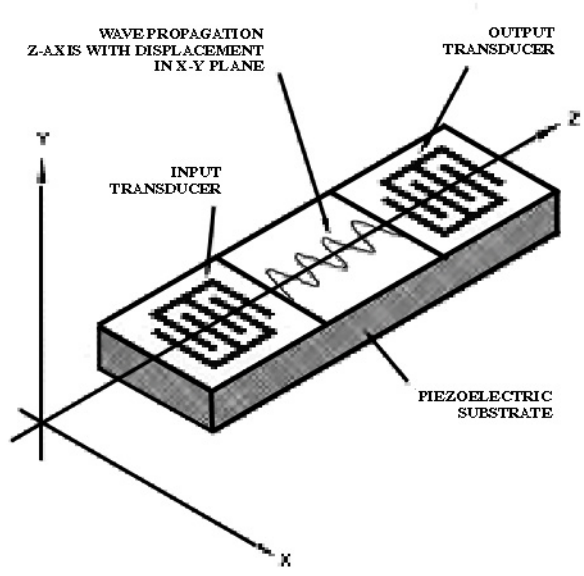

Substrates

AT cut Quartz

Piezoelectric Materials

- **$LiNbO_3$**
- **$LiTaO_3$**
- **SiO_2**

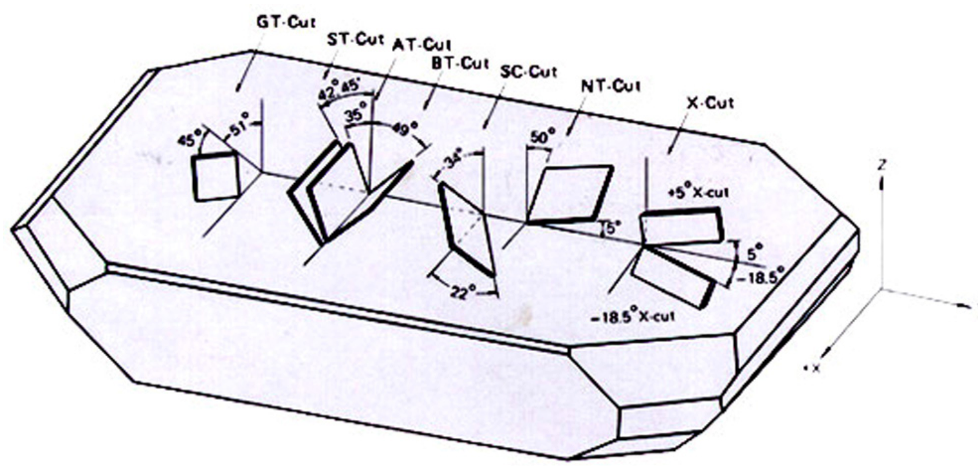

Temperature dependence

Quartz AT cut temperature dependence

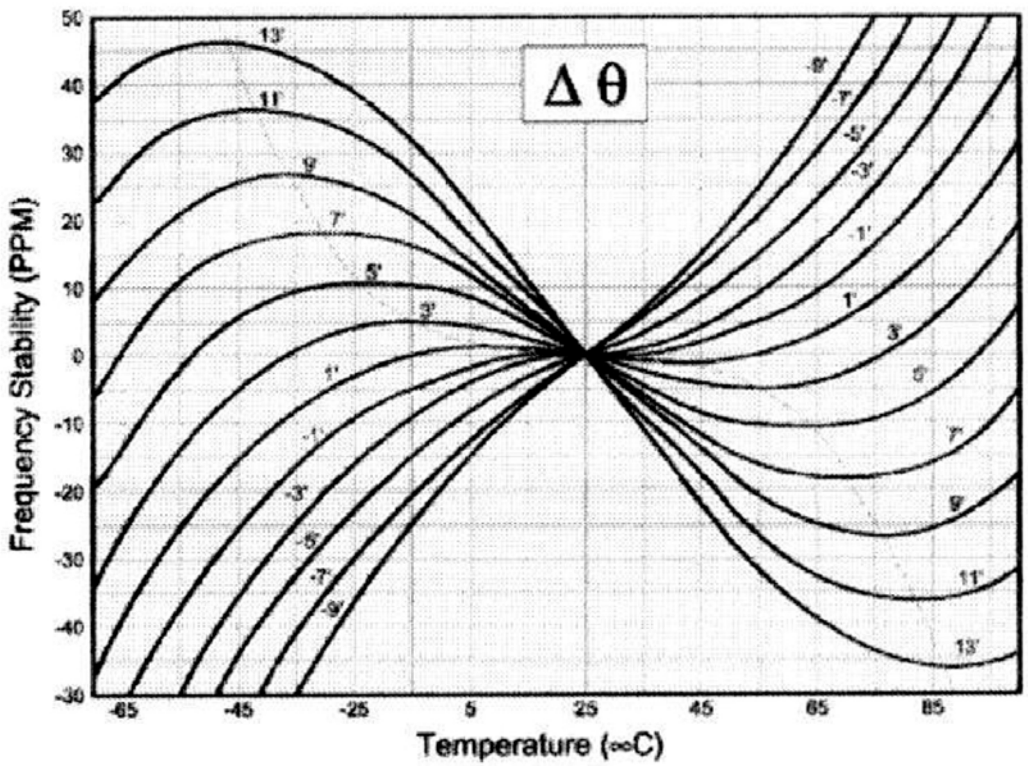

Resonator Layout

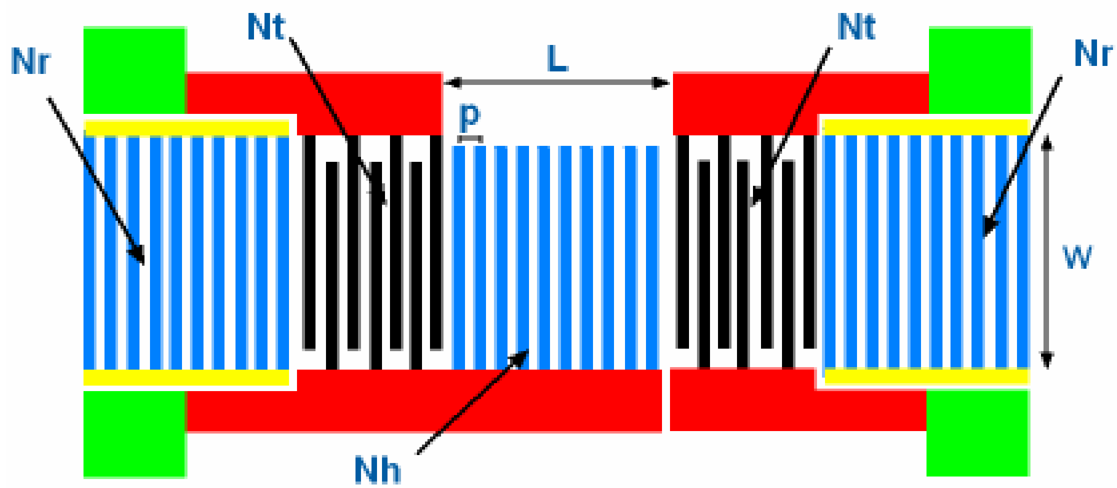

v	p	w	Nt	Nr	Nh	$f_o \propto \frac{v}{2p}$
[m/s]	[µm]	[µm/2p]				[MHz]
5101.471	8	35	80+1/2	480	99	316.36

Some Theory

Waves propagation on periodically perturbed substrates

Consider a substrate with a periodic grating of period p. An incident wave, with a wavelenght double the period p, shows a strong attenuation.

Bragg condition $\lambda = 2p$ $\Rightarrow$ Strong reflection

In this particular condition, reflected waves on each strip of the periodic grating are with the same phase and sum toghether. This leads, when the number of strips is sufficient to a total reflection and this is what is called the "stopband" phenomena.

In order to model this propagation phenomena, we need to start from the classic prpagation equation i.e. the Mathieu equation.

$$\left(\frac{d^2}{dx^2} + k_0^2\right)\varphi(x) = -\zeta(x) k_0^2 \varphi(x)$$

v_0 is the propagation velocity in the unperturbed matter

$k_0 = \frac{\omega}{v_0}$ is the wave number in the unperturbed matter

$\zeta(x) = \zeta_0 - 2\zeta_1 \cos\left(2\pi \frac{x}{p} - \vartheta_r\right)$ is the periodic perturbation, of period p, over x

ζ_1 Amplitude

ϑ_r Initial phase

ζ_0 Offset (uniform mass load)

Some Theory

The general solution is the sum of an infinite number of harmonics called the Floquet harmonics:

$$\varphi(x) = \sum_{n=-\infty}^{+\infty} A_n e^{-\iota\left(\beta + \frac{2\pi n}{p}\right)x} = \sum_{n=-\infty}^{+\infty} A_n e^{-\iota\beta_n x}$$

In order to get the guided modes (values of β corresponding to waves that propagate in the matter) we need to search for the eigenvalues of the system of equations obtained substituting the general solution in the Mathieu, i.e. we have to solve the "dispersion equation". This system has unfortunately an infinite number of equation. Thus, we need to approximate the general solution with a finite number of terms.

Coupled Modes Theory (COM)

Assuming a weak perturbation ($|\zeta_1| << 1$) and limiting the analysis near the Bragg condition ($f_0 = \frac{v}{2p}$), it could be verified that the harmonics n=0 and n=-1 are dominant. Furthermore, the two harmonics are coupled; they have the same propagation constant but opposite verse:

$$\beta_0 = \frac{2\pi}{\lambda} \cong \frac{\pi}{p} \qquad \beta_{-1} = \beta_0 - \frac{2\pi}{p} \cong -\beta_0$$

Thus, we could simplify imposing: $\beta_0 = \frac{\pi}{p} + q \qquad \beta_{-1} = -\frac{\pi}{p} + q \qquad |q| << \frac{\pi}{p}$

and obtaing a general solution of the form: $\varphi(x) = A_0 e^{-\iota q x} e^{-\iota\frac{\pi}{p}x} + A_{-1} e^{-\iota q x} e^{+\iota\frac{\pi}{p}x} \qquad \Rightarrow$

$$\varphi(x) = A^+(x) e^{-\iota\frac{\pi}{p}x} + A^-(x) e^{+\iota\frac{\pi}{p}x} \qquad \begin{cases} A^+(x) = A_0 e^{-\iota q x} \\ A^-(x) = A_{-1} e^{-\iota q x} \end{cases}$$

Some Theory

The dispersion equation

$$\begin{cases} \dfrac{d}{dx}A^+(x) = -\imath\delta A^+(x) + \imath k A^-(x) \\ \dfrac{d}{dx}A^-(x) = -\imath k^* A^+(x) + \imath\delta A^-(x) \end{cases}$$

$$\delta = \frac{2\pi(f - f_0)}{v}$$ parametro di detuning

$$k = \frac{\zeta_1 p}{2\pi} k_0^2 e^{\imath\vartheta_r}$$ parametro di coupling

$$\Downarrow$$

$$q = \pm\sqrt{\delta^2 - |k|^2} \qquad \mathrm{Im}(q) \leq 0$$

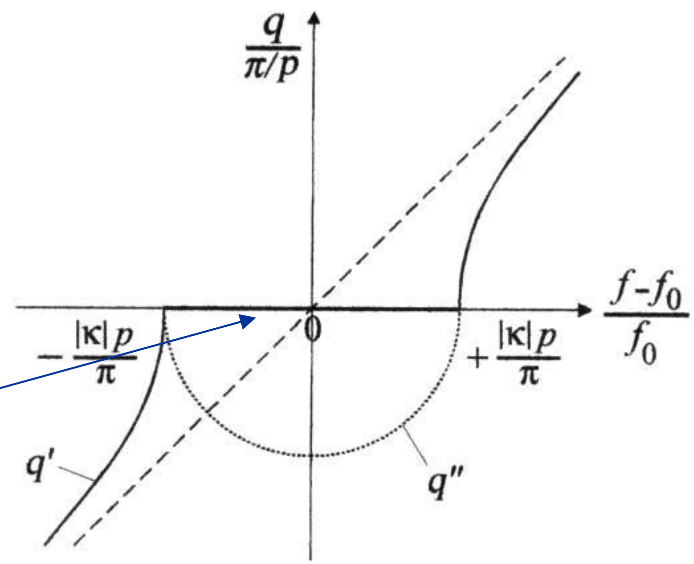

Vanishing waves
“Stopband”

Some Theory

The dispersion equation for the STW modes

$$q = \sqrt{\Delta^2 - \frac{1}{4}\left(|\varepsilon|^2 \pm \eta\sqrt{2|\varepsilon|^2 - \eta^2 - 4\Delta}\right)^2}$$

Plessky, Abbot and Hashimoto

V. Plessky – J. Koskela, "Coupling of mode analysis of SAW devices", International Journal of High Speed Electronics and Systems

V. Plessky, "A Two Parameter COM model for Shear Horizontal Type Propagation in Periodic Gratings", Proc. IEEE Ultrason. Symp. (1993) 195-200

B. Abbot - K. Hashimoto, "A Coupling of modes Formalism for Surface Transverse Wave Devices", Proc. IEEE Ultrason. Symp. (1995) 239-245

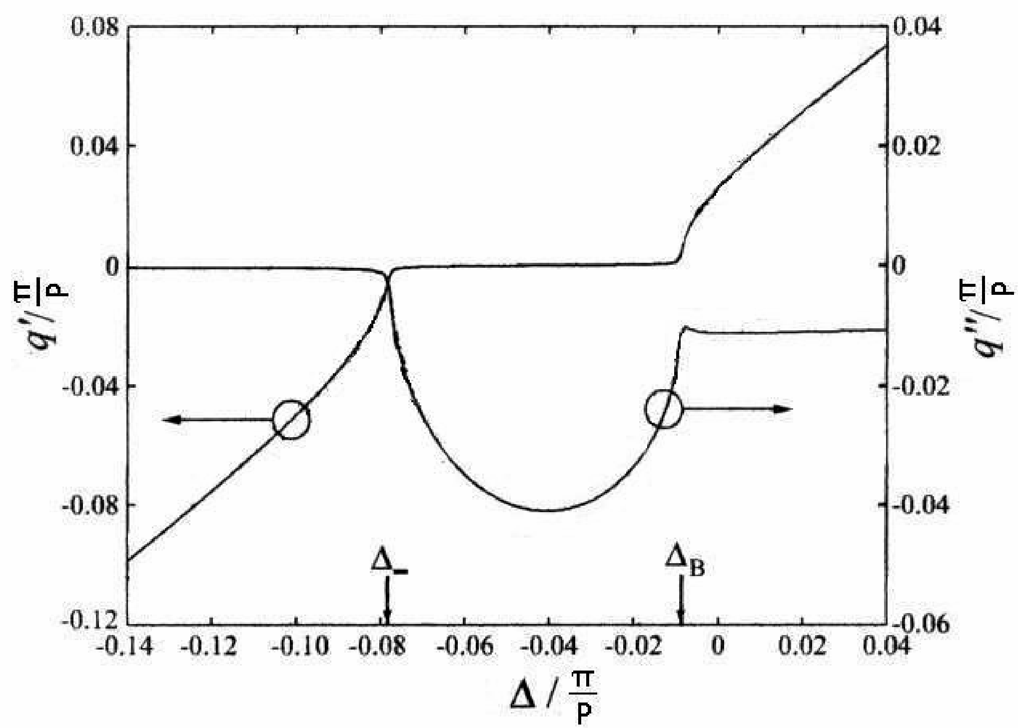

Some Theory

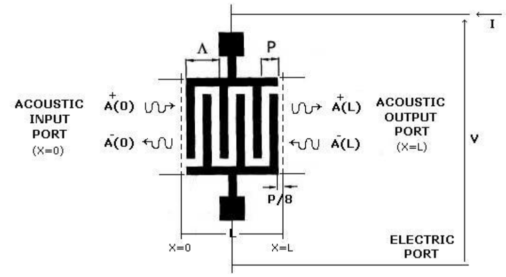

ACOUSTIC INPUT PORT (X=0)
ACOUSTIC OUTPUT PORT (X=L)
ELECTRIC PORT
Λ
P
P/8
L
X=0
X=L
I
V

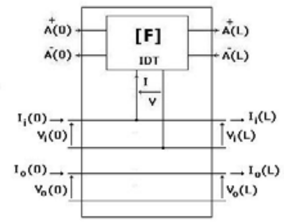

[F]
IDT

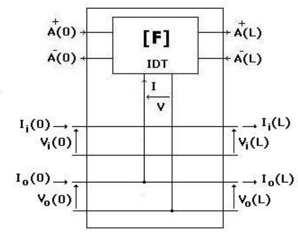

[F]
IDT

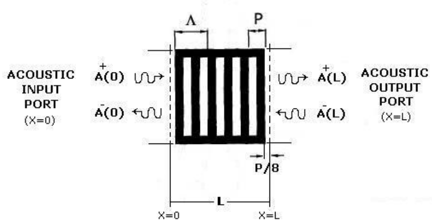

ACOUSTIC INPUT PORT (X=0)
ACOUSTIC OUTPUT PORT (X=L)
Λ
P
P/8
L
X=0
X=L

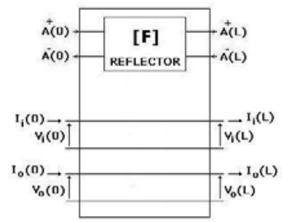

[F]
REFLECTOR

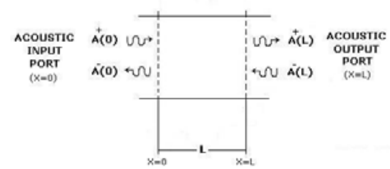

ACOUSTIC INPUT PORT (X=0)
ACOUSTIC OUTPUT PORT (X=L)
L
X=0
X=L

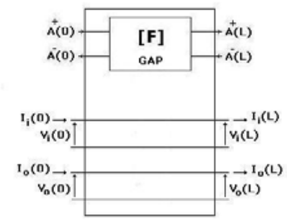

[F]
GAP

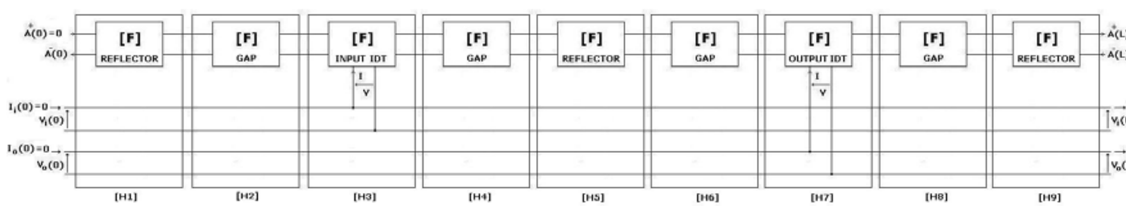

[F]
REFLECTOR
GAP
INPUT IDT
OUTPUT IDT
[H1]
[H2]
[H3]
[H4]
[H5]
[H6]
[H7]
[H8]
[H9]

The simulator

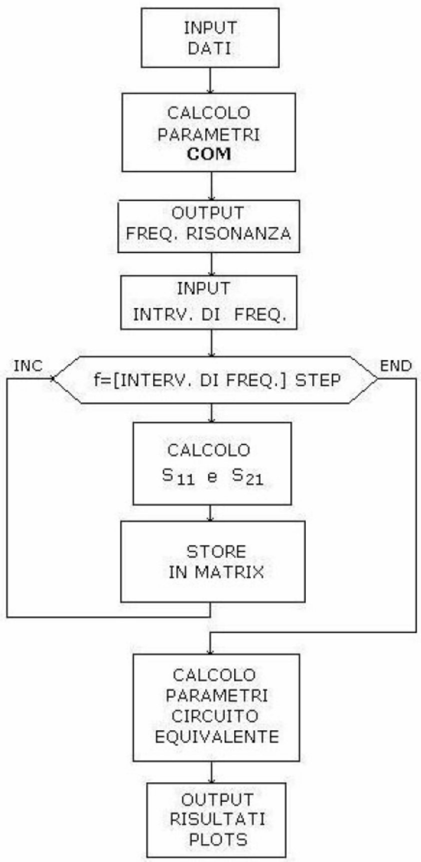

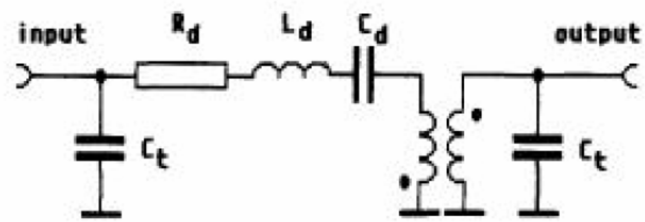

$$Q_{LOADED} = \frac{f_0}{BW_{3dB}}$$

$$Q_{UNLOADED} = \frac{Q_{LOADED}}{\left(1-10^{\frac{IL}{10}}\right)}$$

$$R_d = \frac{100 Q_{LOADED}}{Q_{UNLOADED} - Q_{LOADED}}$$

$$L_d = \frac{R_d Q_{UNLOADED}}{2\pi f_0}$$

$$C_d = \frac{1}{(2\pi f_0)^2 L_d}$$

Resonator Layout

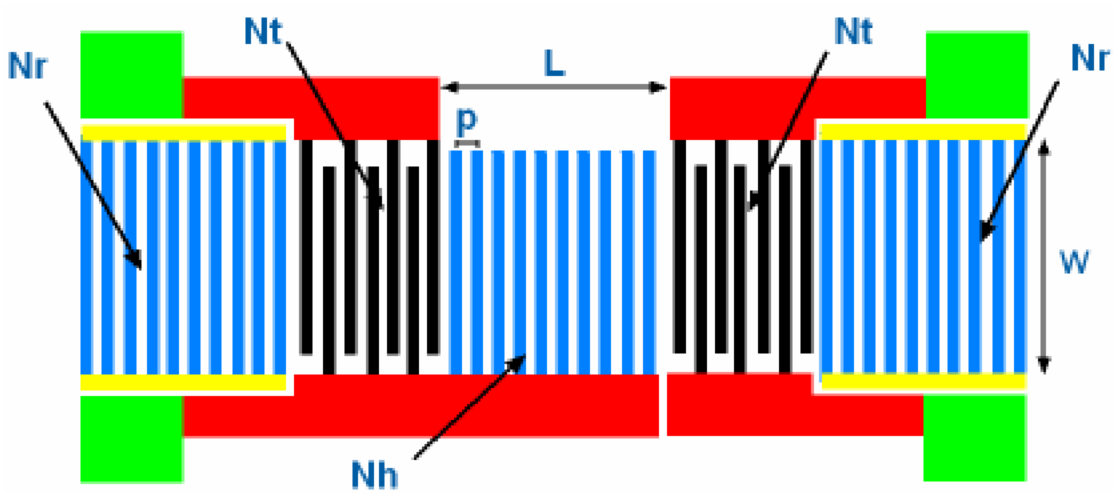

v	p	w	Nt	Nr	Nh	$f_o \propto \frac{v}{2p}$
[m/s]	[μm]	[μm/2p]				[MHz]
5101.471	8	35	80+1/2	480	99	316.36

Resonator Layout

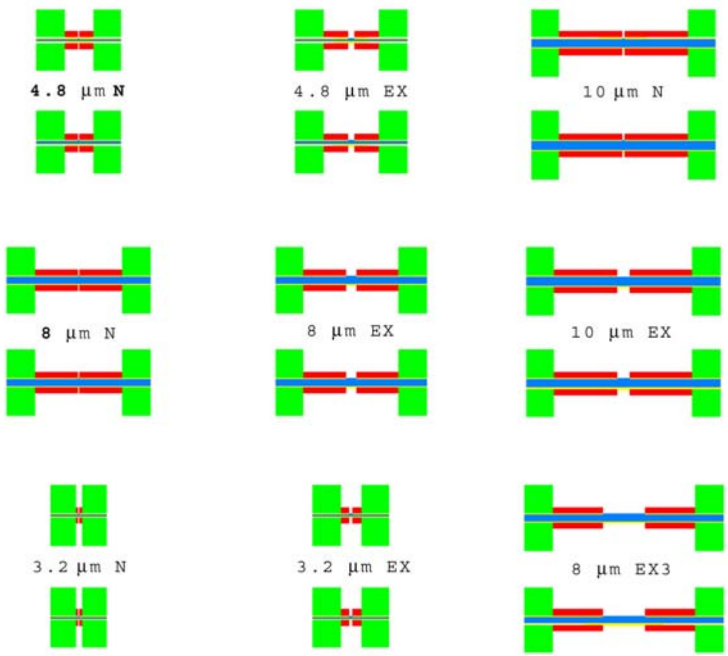

Designed patterns

	Nr	Nt	Nh	w	a	fo [MHz]
8 µm N	480	161	25	35	50	316
8 µm EX	480	161	99	35	50	316
8 µm EX3	480	161	400	35	50	316
10 µm N	500	161	25	35	50	253
10 µm EX	500	161	99	35	50	253
4.8 µm N	450	181	25	30	50	520
4.8 µm EX	600	201	99	30	50	520
3.2 µm N	450	181	25	30	50	782
3.2 µm EX	600	221	99	30	50	782

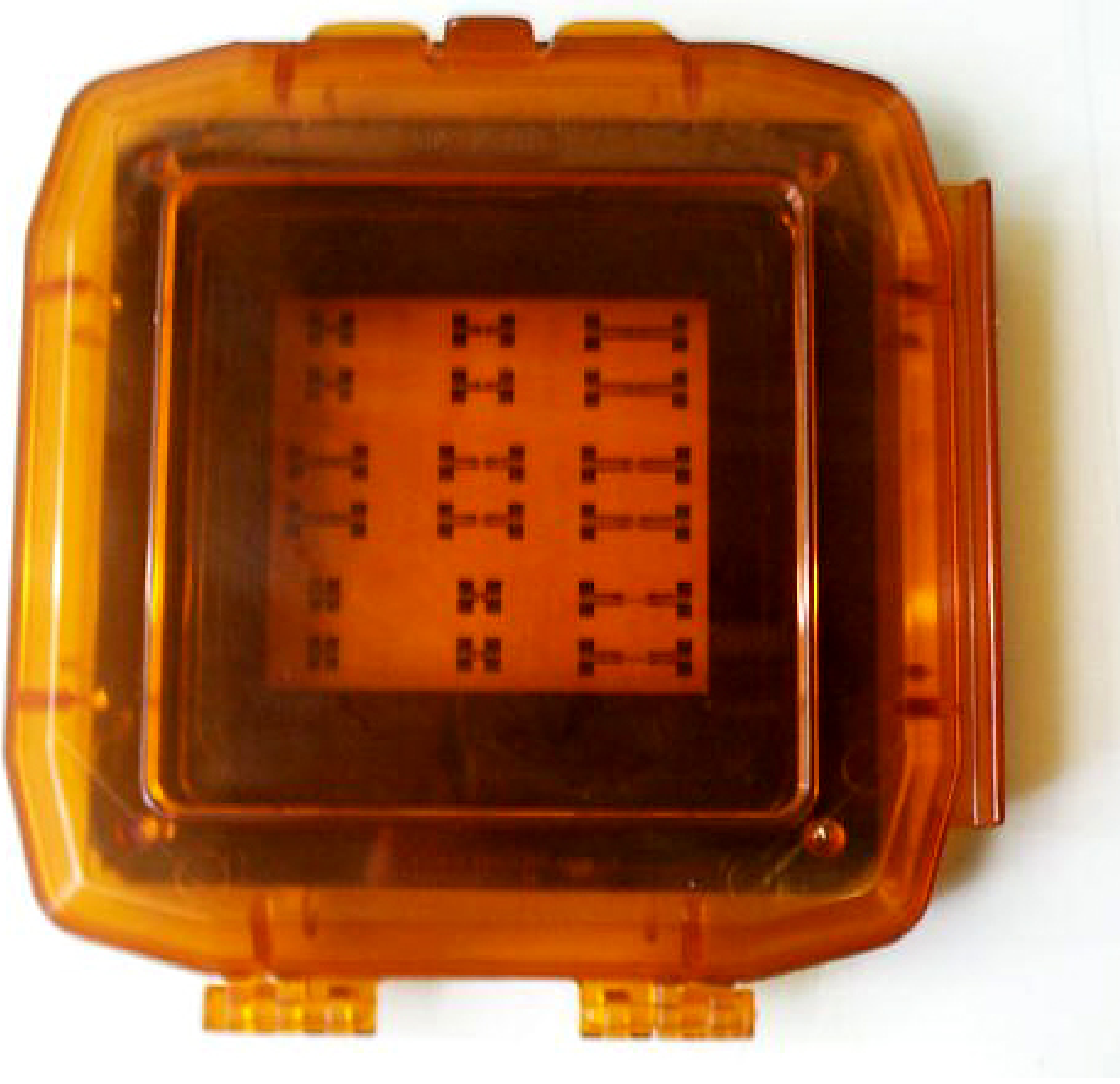

Resonator Layout

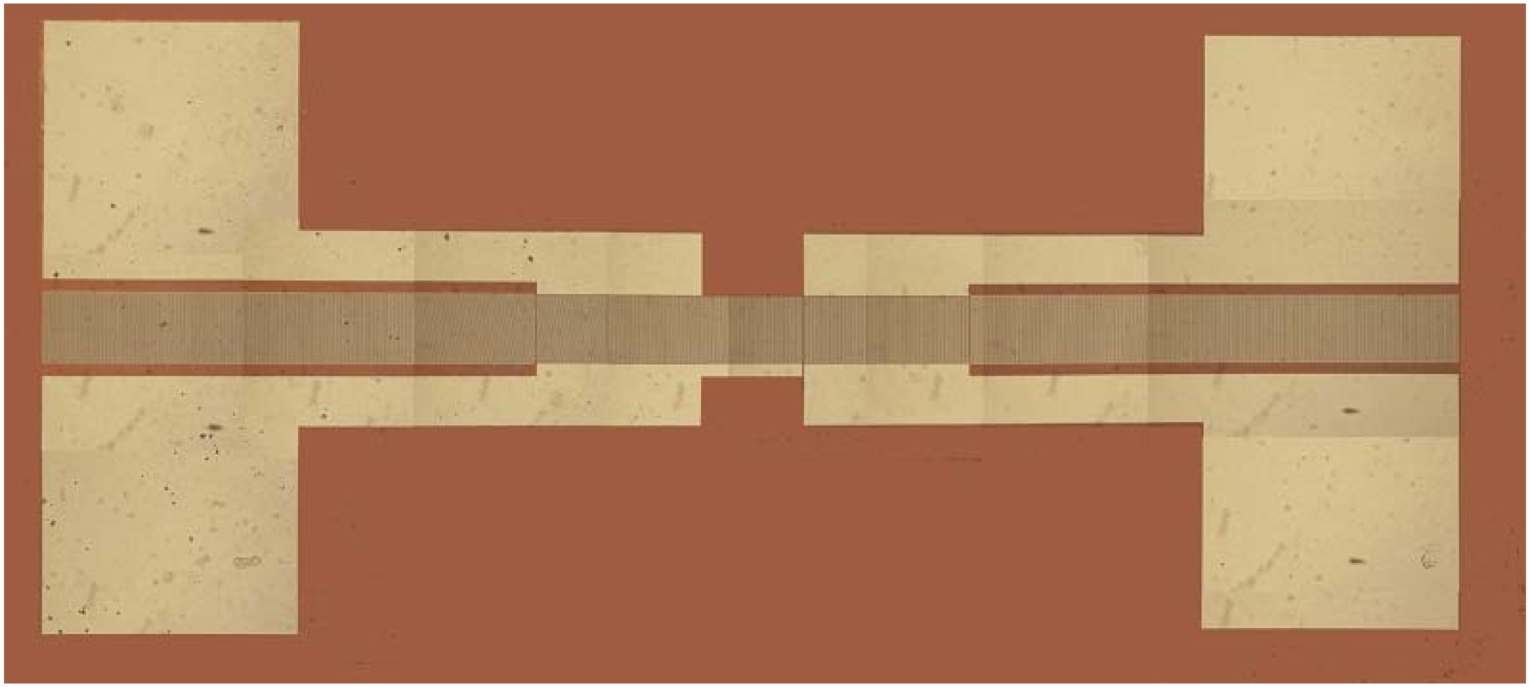

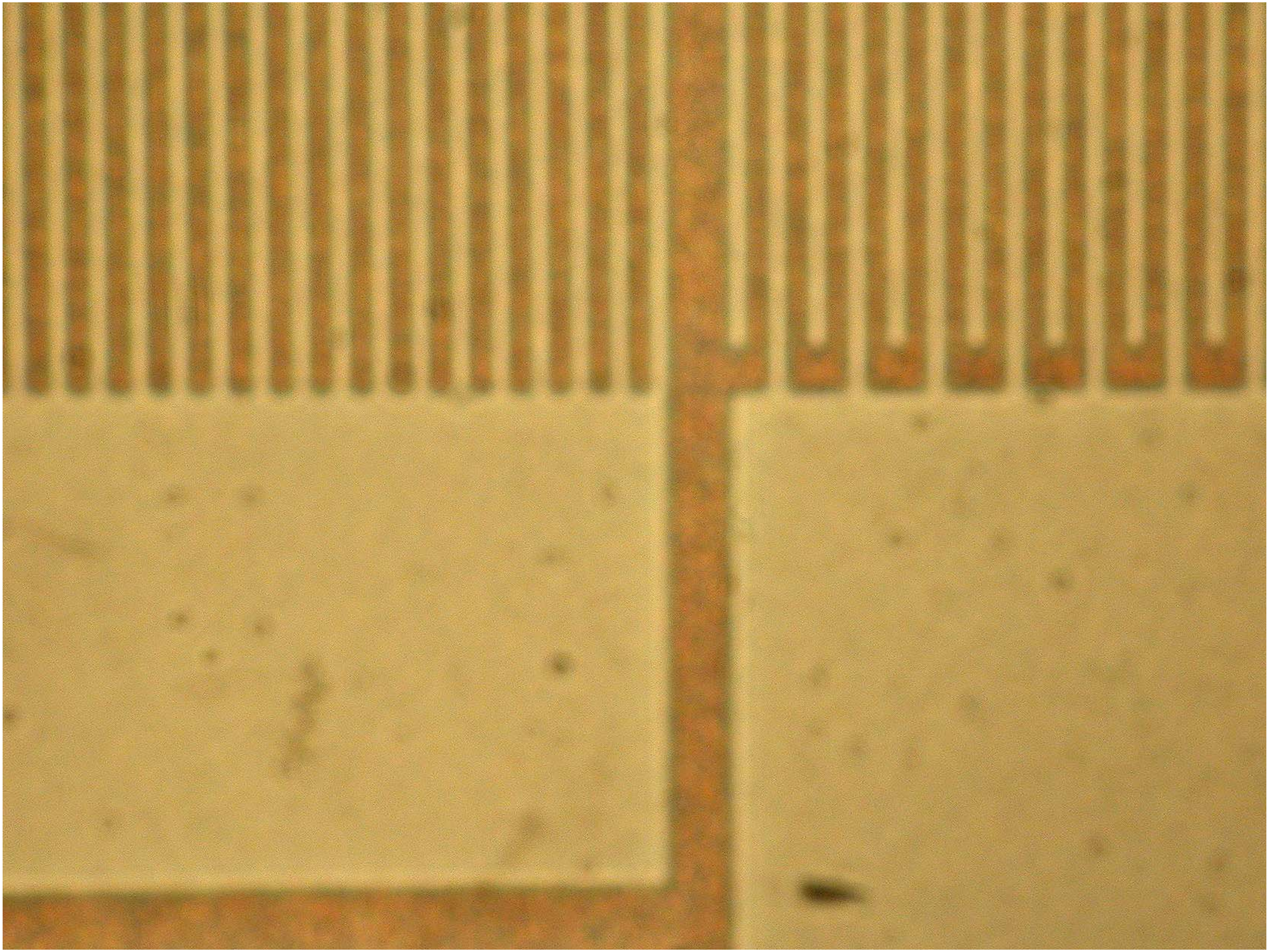

Frequency Response

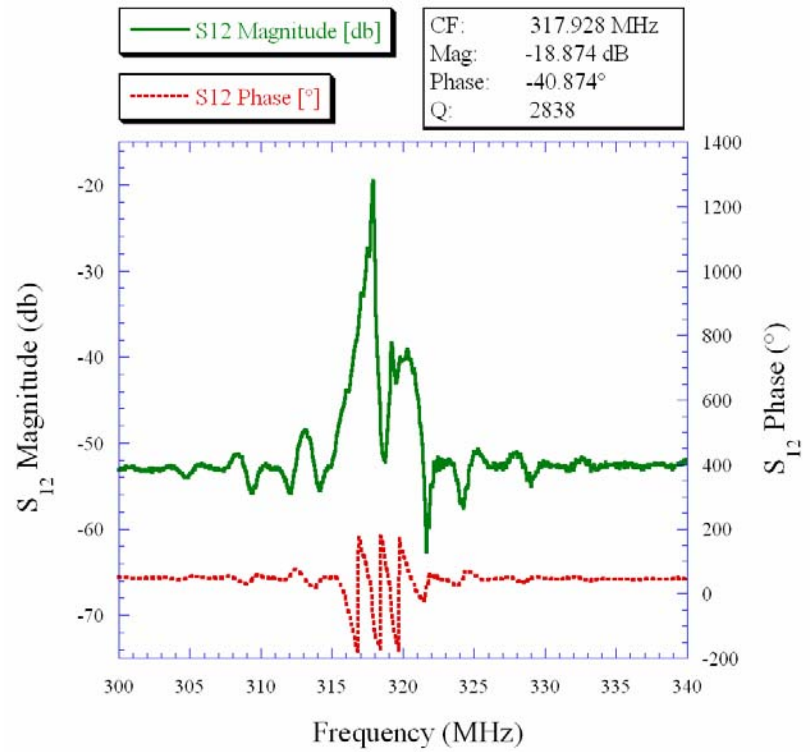

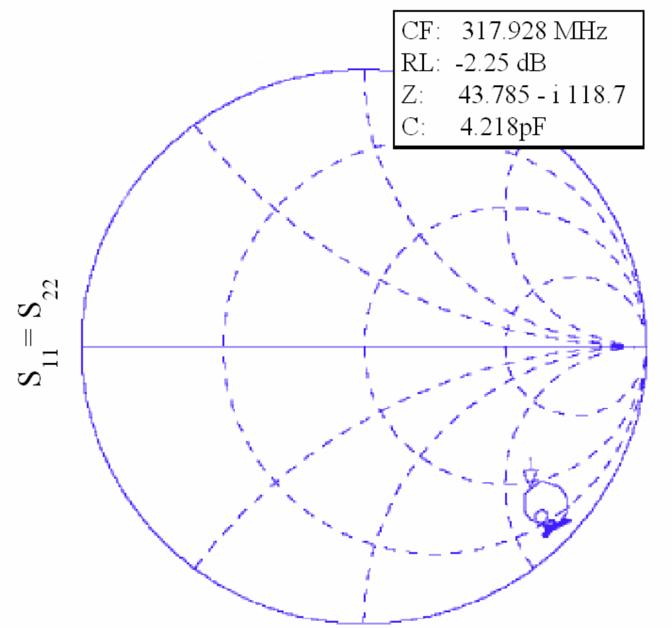

Frequency range: [300-340] (MHz)

Comparison of the results

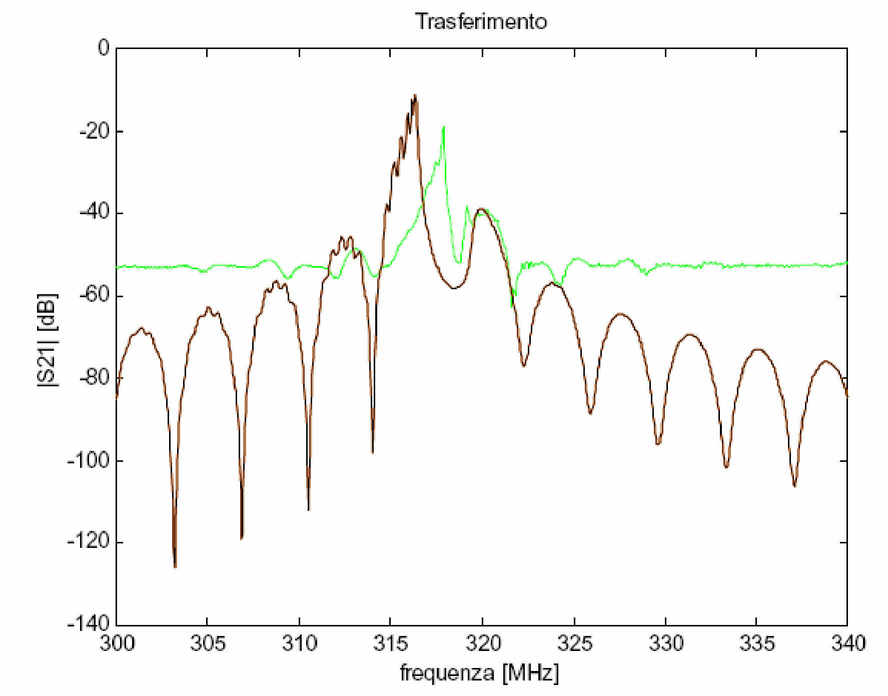

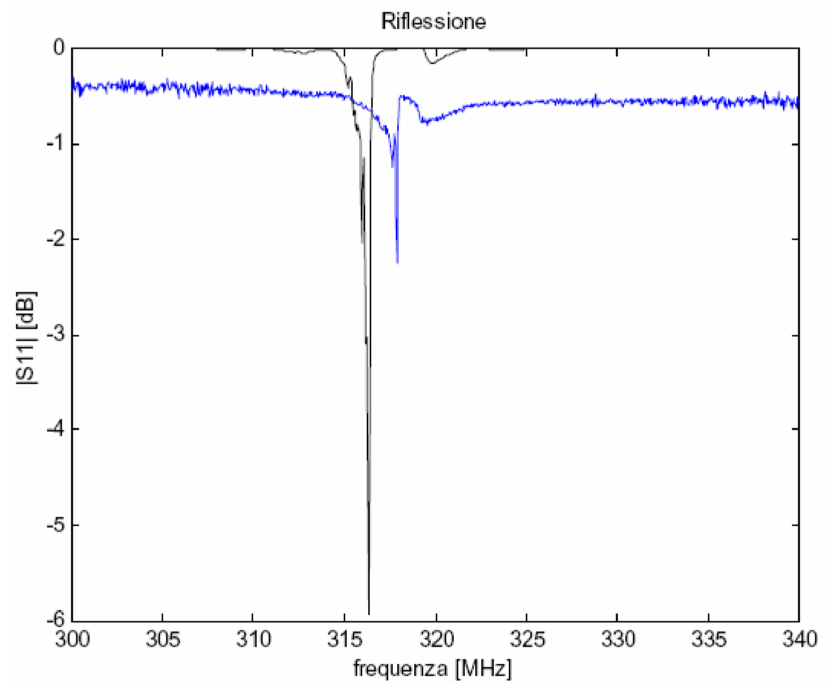

Polymers

PECVD

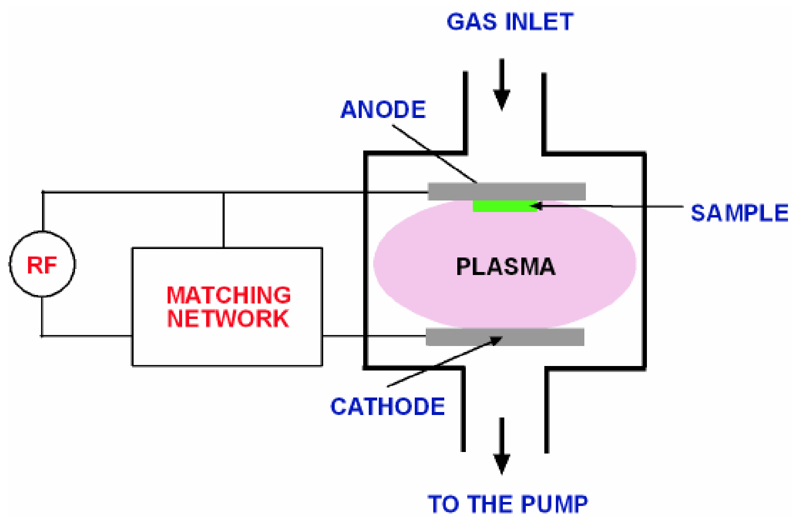

Deposition Parameters

	Gas mixture	Pressure	P_{RF}	Time	Thickness
HMDSO	HMDSO(33%)/O_2	50 mTorr	100 W	10 min	320 nm
a-C:H dev.1	CH_4(5%)/Ar	300 mTorr	250 W	30 min	430 nm
a-C:H dev.2	CH_4(21.5%)/Ar	300 mTorr	250 W	30 min	440 nm
a-C:H dev.3	CH_4(50%)/Ar	300 mTorr	250 W	30 min	380 nm
a-C:H dev.4	CH_4(90%)/Ar	300 mTorr	250 W	30 min	340 nm
a-C:H dev.5	CH_4(100%)	300 mTorr	250 W	30 min	350 nm

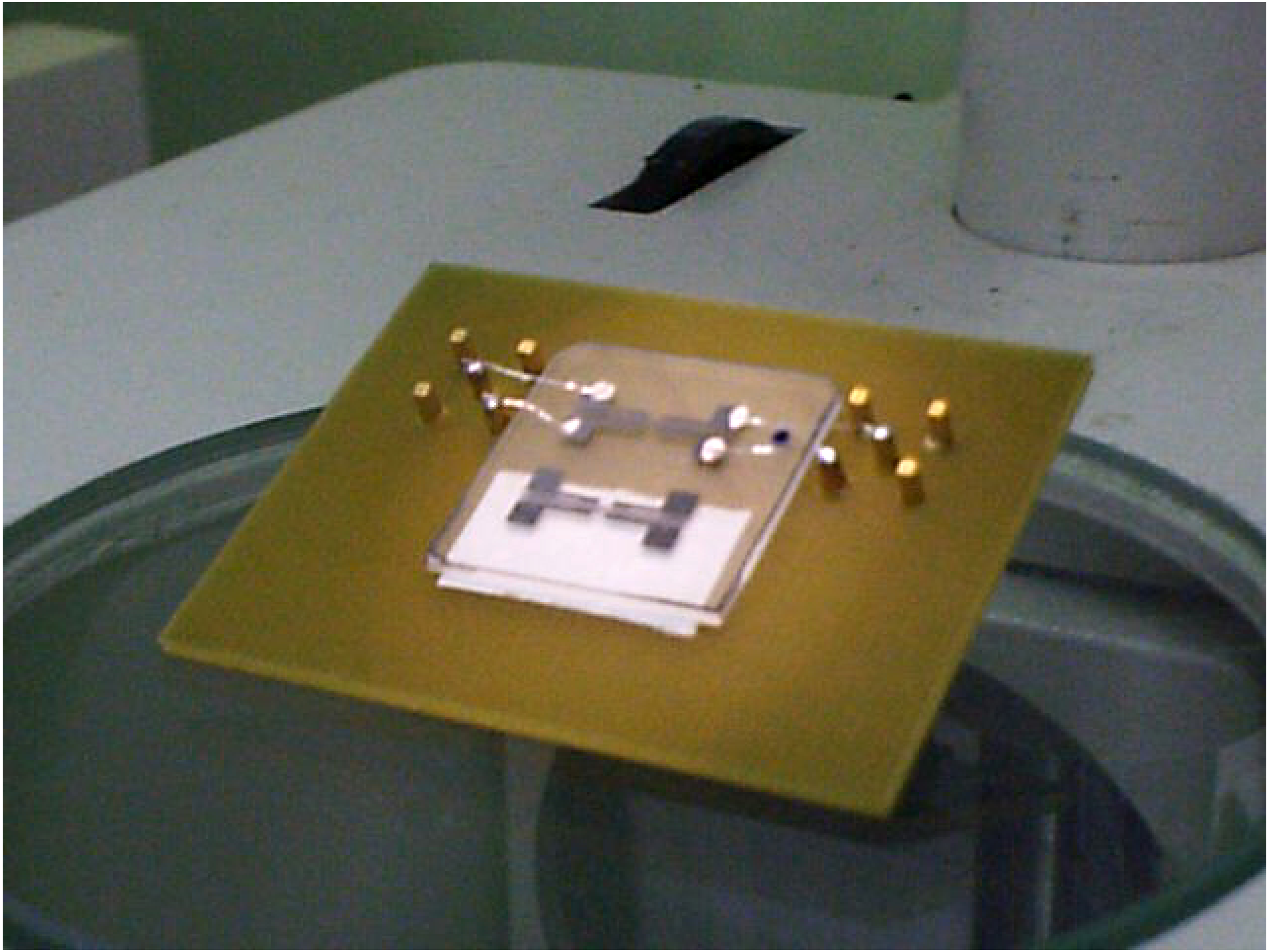

Outline

- A sensor for high relative humidity ranges
- How does our sensor work?
  - The acoustic device
  - The sensing mechanism
- Experiment set-up
- Results
- Front-end electronics
- Conclusions

Experiment set-up

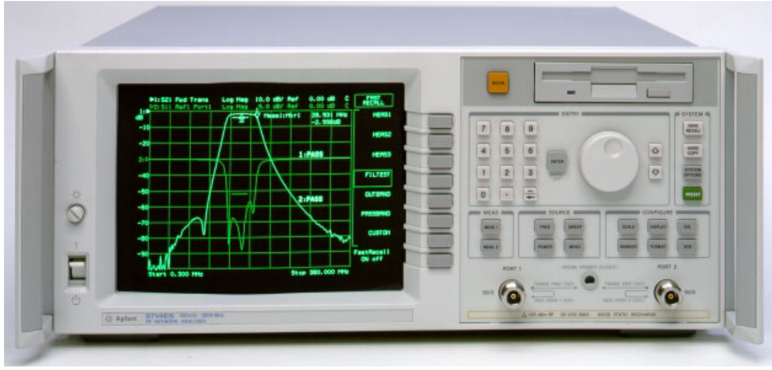

- Climatic Chamber Mazzali Climatest C 330 G5
- Agilent 8714ET RF network analyzer
- Solomat MPM 500e chilled mirror sensor equipped with 355RH probe

$$Rel.\ Freq.\ shift(x\%\ RH) = \frac{Reson.\ freq.(x\%\ RH) - Reson.\ freq.(100\%\ RH)}{Reson.\ freq.(100\%\ RH)} x10^6$$

Outline

- A sensor for high relative humidity ranges
- How does our sensor work?
  - The acoustic device
  - The sensing mechanism
- Experiment set-up
- Results
- Front-end electronics
- Conclusions

Resonance Frequency Down-shift

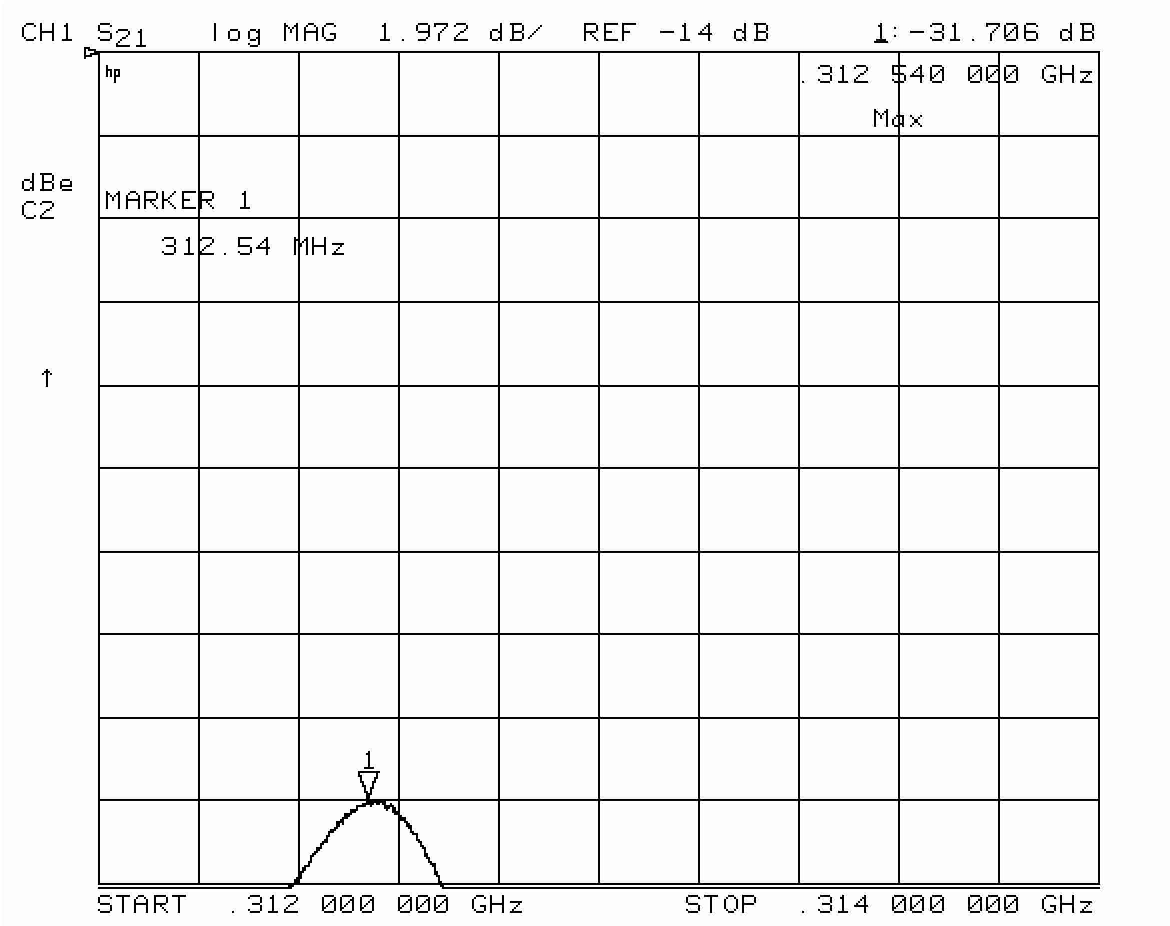

Sensitivity

HFC (Humidity Frequency Characteristic)

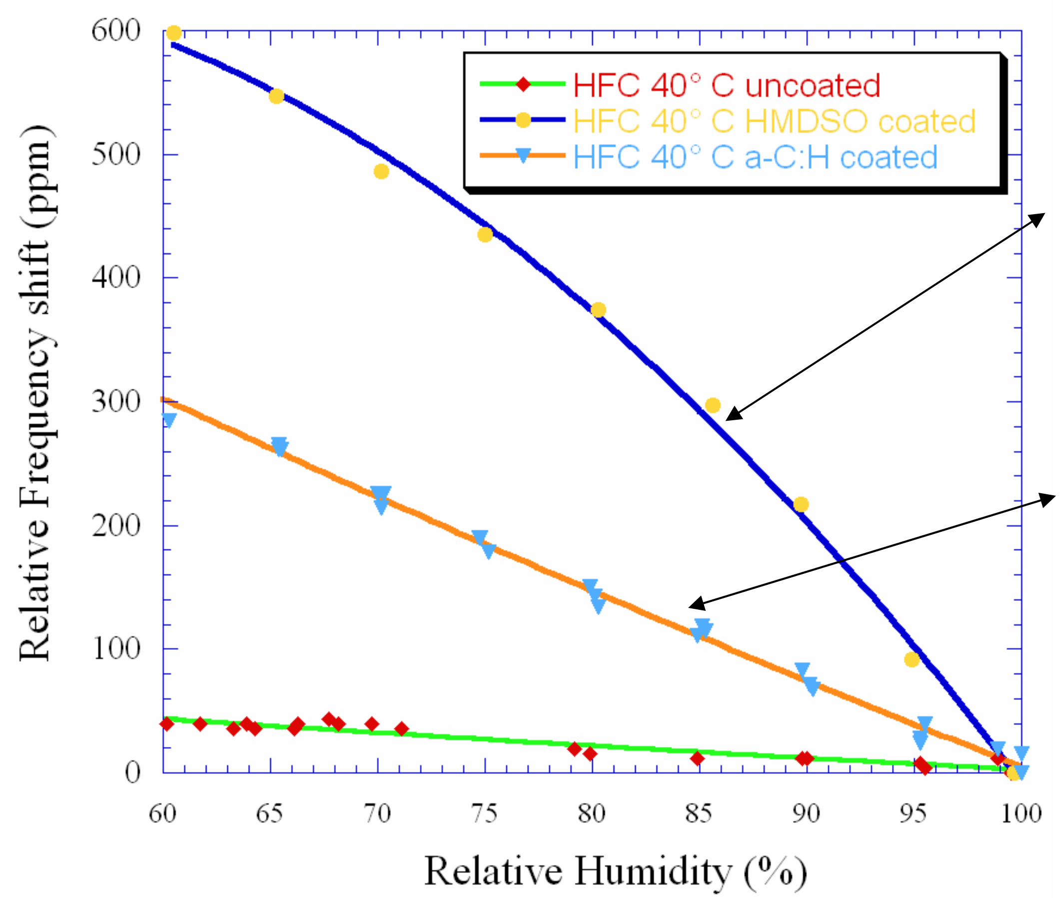

HMDSO

Mean sensitivity 15 ppm/%RH

(absolute freq. shift of 4.5 kHz/%RH)

a-C:H

Mean sensitivity 7.5 ppm/%RH

(absolute freq. shift of 2.25 kHz/%RH)

Changing CH_4 percentages

HFC (Humidity Frequency Characteristic)

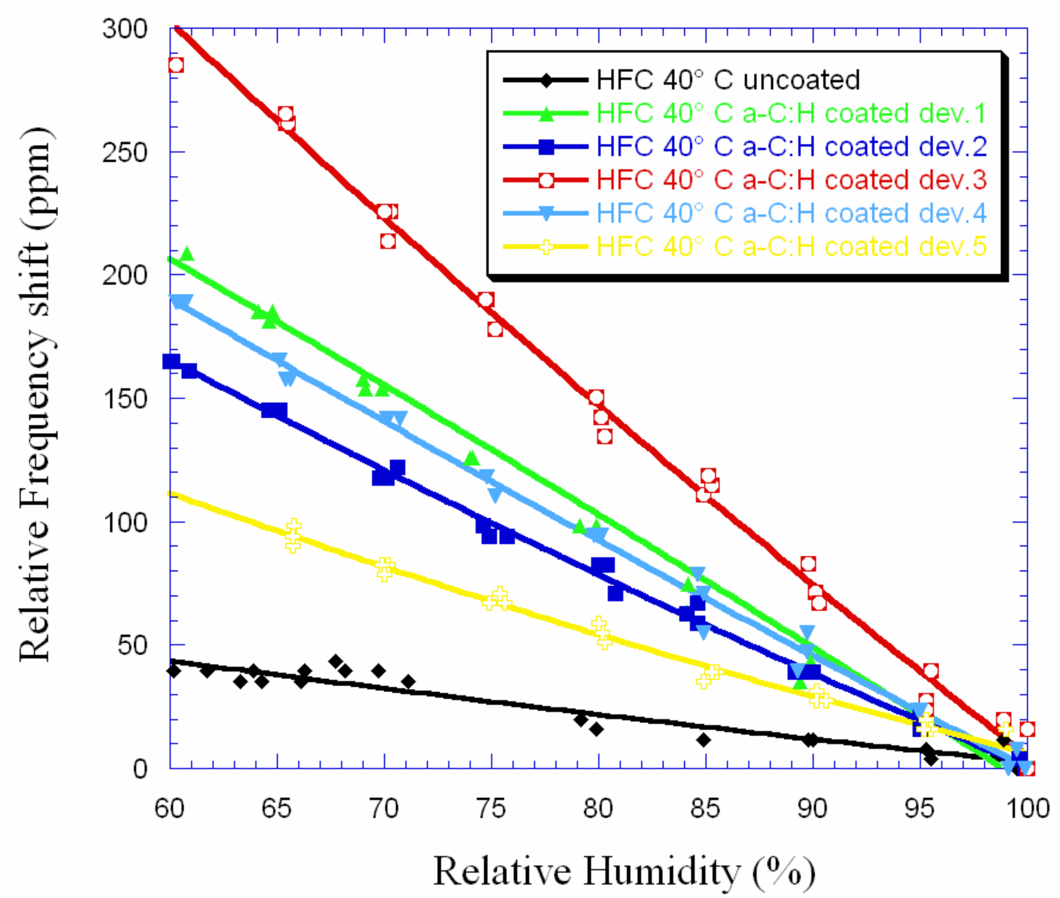

CH_4 percentages

a-C:H dev.1	CH_4(5%)/Ar
a-C:H dev.2	CH_4(21.5%)/Ar
a-C:H dev.3	CH_4(50%)/Ar
a-C:H dev.4	CH_4(90%)/Ar
a-C:H dev.5	CH_4(100%)

Changing CH_4 percentages

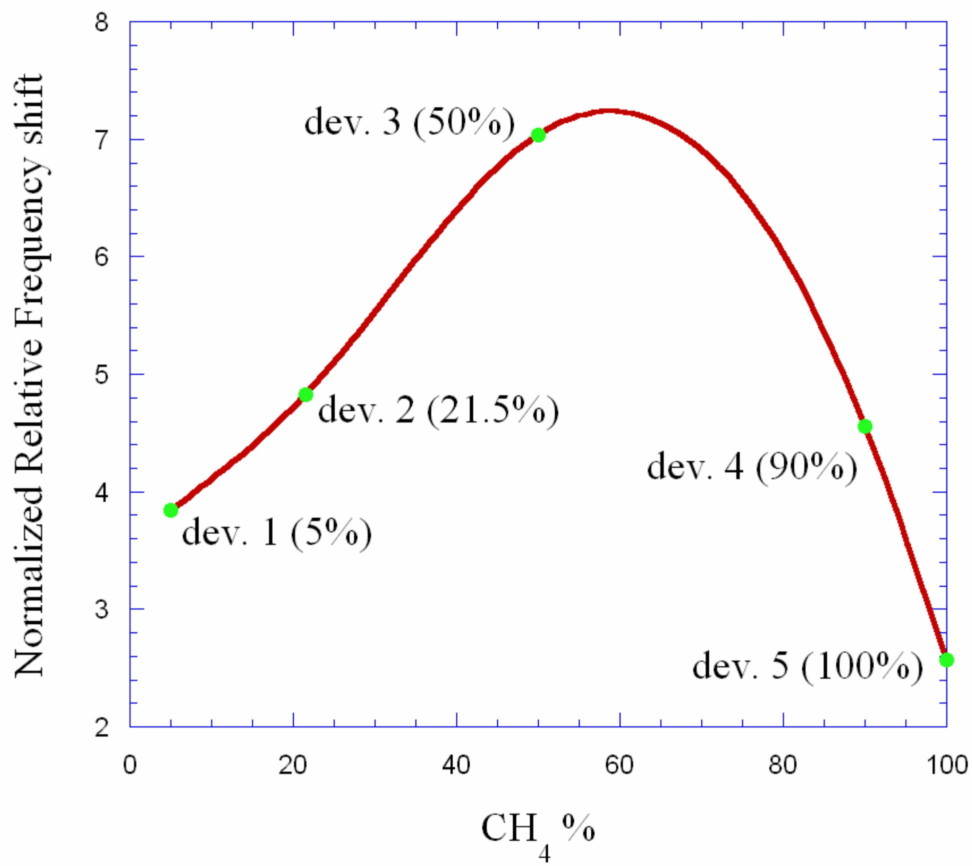

HFC hysteresis

Hysteresis of HMDSO coated STW resonator

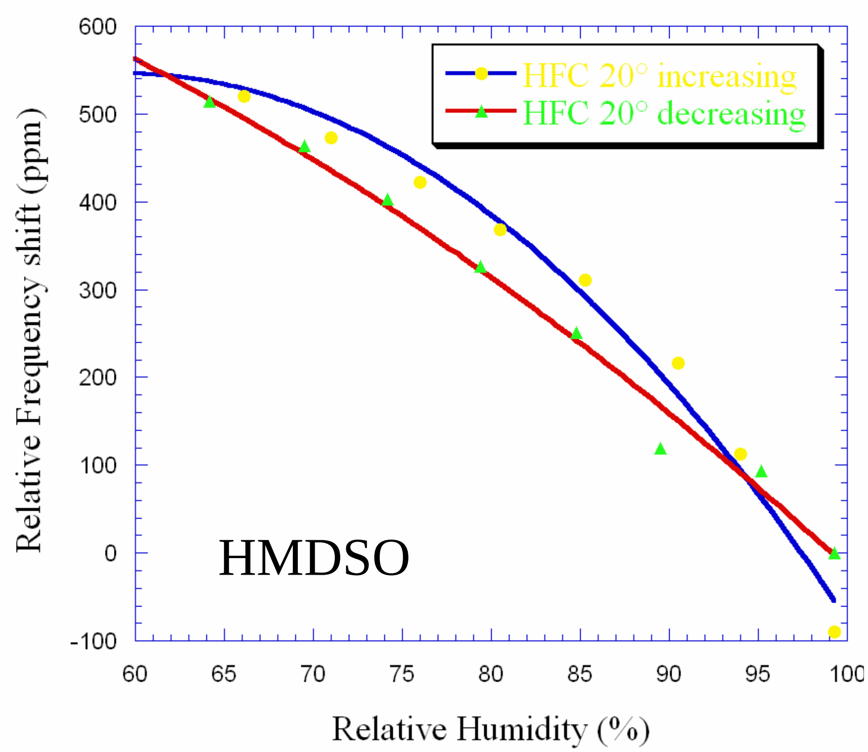

Hysteresis of a-C:H coated STW resonator

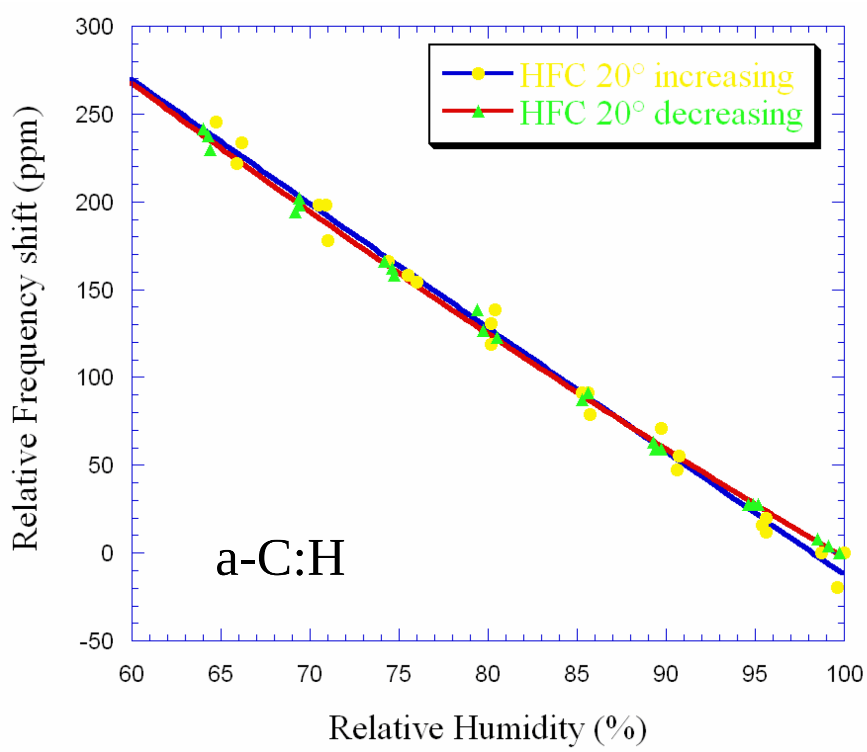

Temperature dependence

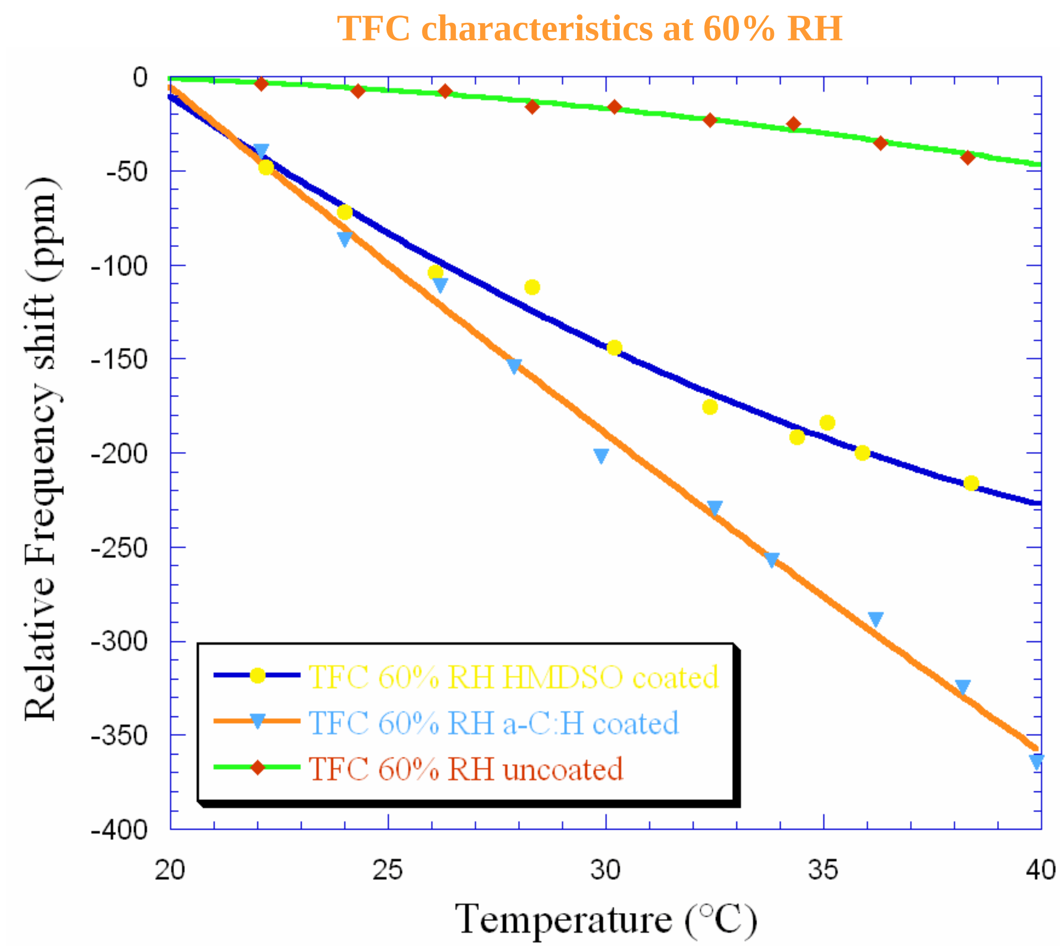

Response Time

Response time to a pulse of 90% RH

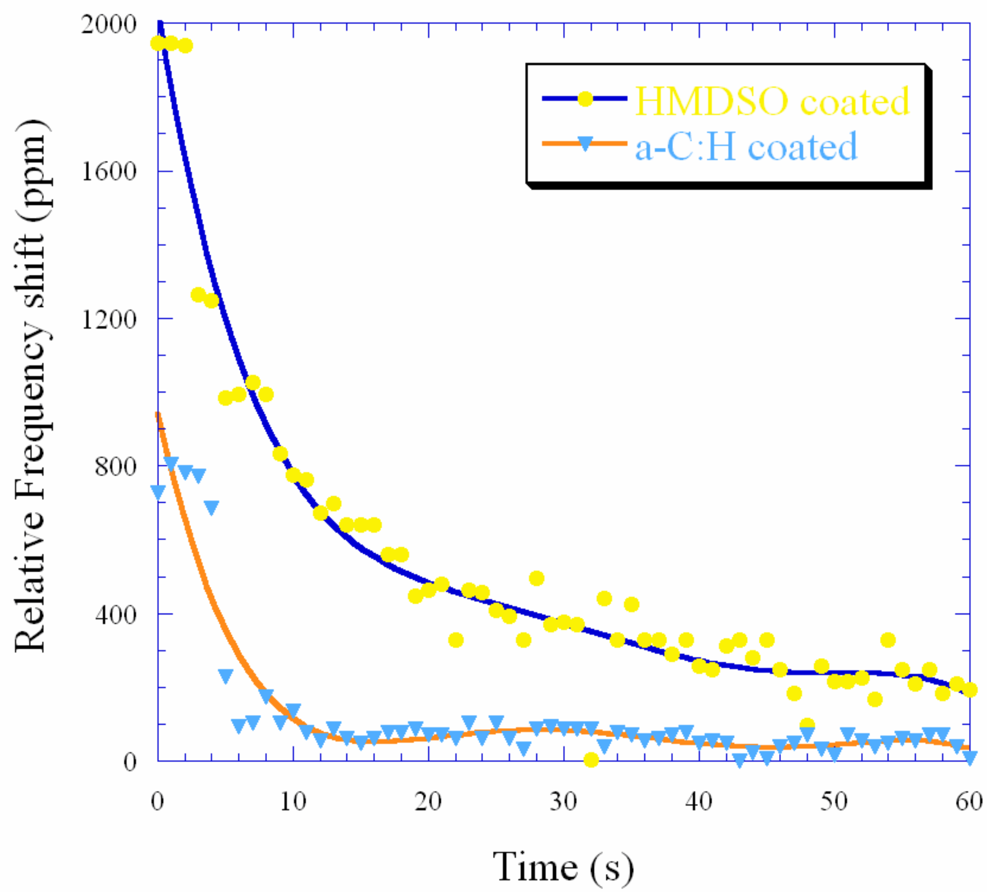

Outline

- A sensor for high relative humidity ranges
- How does our sensor work?
  - The acoustic device
  - The sensing mechanism
- Experiment set-up
- Results
- Front-end electronics
- Conclusions

Electronic Front-end

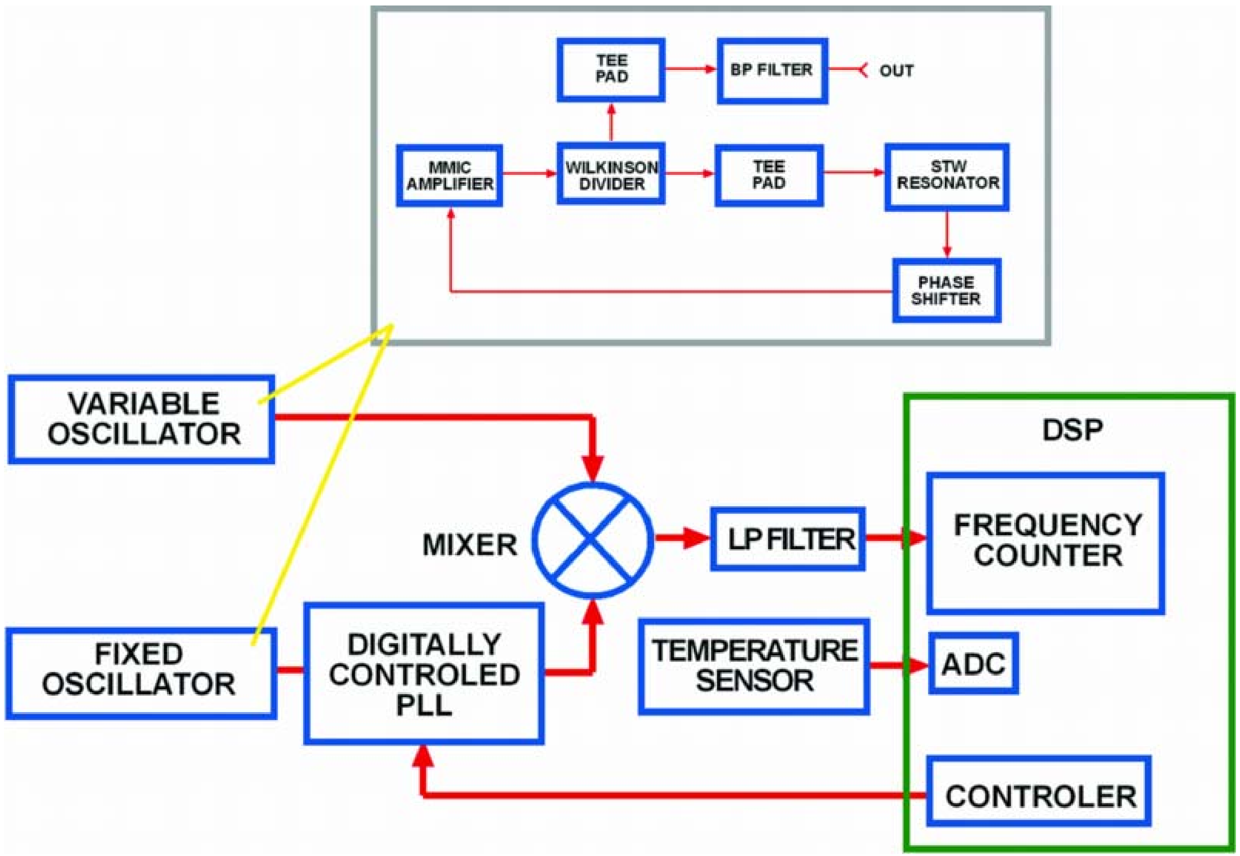

Outline

- A sensor for high relative humidity ranges
- How does our sensor work?
  - The acoustic device
  - The sensing mechanism
- Experiment set-up
- Results
- Front-end electronics
- Conclusions

Conclusions

a. Polymer-coated surface transverse acoustic wave humidity sensors have been successfully fabricated and characterized.

b. Different kinds of polymeric films, HMDSO and a-C:H, deposited at room temperature by PECVD, have been tested and their sensing characteristics have been compared.

c. At room temperature average sensitivities of 15 ppm/%RH and 7.5 ppm/%RH have been obtained for HMDSO and a-C:H films, respectively, which have been found to be about one order of magnitude and three times higher than results reported in literature.

d. The a-C:H coated STW resonator features a fast response time (10s) and a linear and hysteresis-free HFC characteristics, in spite of a lower sensitivity and a higher temperature dependence with respect to HMDSO coated one.

e. A compensation by signal processor controlled oscillator system is needed to reduce temperature dependence.

Some literature

[1] G. Cicala, P. Bruno, **A. Dragone**, A.M. Losacco, C. Sadun, A. Generosi, ‘Characteristic Of PECVD a-C:H films suitable for STW resonant devices’, to appear on *Thin Solid Films.*

[2] P. Bruno, G. Cicala, F. Corsi, **A. Dragone**, A.M. Losacco**,** ‘High relative humidity range sensor based on polymer-coated STW resonant device’**,** *Sensors and Actuators B*, 100 (2004) p.126.

[3] F. Corsi, **A. Dragone**, A. M. Losacco: "Primo premio Design In Award 2003 - Un sistema di controllo per le nebbie fredde", Design-In Maggio 2003.

[4] F. Corsi, **A. Dragone**, A. M. Losacco: "Un sistema di controllo per le nebbie fredde", Design-In Marzo 2003

[5] F. Corsi, **A. Dragone**, A. M. Losacco: "High resolution humidity sensor based on STW resonant device", Sensors and Microsystems - Proceedings of the 8th Italian Conference, Trento, Italy 12 - 14 February 2003, ISBN 981-238-747-1 p.170.

[6] Z.M. Rittersma, *Sensors and Actuators A* 96 (2002) 196.

[7] C. Caliendo, E. Verona, A. D’Amico, A. Furlani, G. Iucci, M.V. Russo, *Sensors and Actuators B* 15-16 (1993) 288

[8] M.Penza, G. Cassano, *Sensors and Actuators B* 68 (2000) 300

[9] I.D. Avramov , S. Kurosawa, M. Rapp, P.Krawczak, E.I. Radeva, *IEEE Trans. on Microwave Theory and Techniques* 49 (2001) 827.

[10] I.D. Avramov, *IEEE Trans. Ultrason. Ferroelect. Freq. Control* 40 (1993) 459

[11] K. Y. Hashimoto, M. Yamaguchi, *Proc. IEEE Ultrason. Symp.* (1996) 300.

[12] P. Cross, R. Schmidt, *The Bell System Technical Journal* (1977) 1447.

[13] S. Denisenko, I. D. Avramov, *Proc. IEEE Freq. Control Symp.* (1993) 645

[14] E. Radeva, L.Spassov, *Vacuum* 51 (1998) 217.

[15] E.I. Radeva, I.D. Avramov, *Mater. Sci. & Engineering C* 12 (2000) 71.

Thank you, very much
for your attention.